This is the accepted manuscript made available via CHORUS. The article has been published as:

Oscillating terms in the Renyi entropy of Fermi gases and liquids

Brian Swingle, Jeremy McMinis, and Norm M. Tubman

Phys. Rev. B **87**, 235112 — Published 12 June 2013

DOI: 10.1103/PhysRevB.87.235112

Oscillating terms in the Renyi entropy of Fermi gases and liquids

Brian Swingle
Department of Physics, Harvard University, Cambridge MA 02138

Jeremy McMinis
Department of Physics, University of Illinois at Urbana Champaign, Urbana IL 61820
Lawrence Livermore National Laboratory, Livermore CA 94550

Norm M. Tubman
Department of Physics, University of Illinois at Urbana Champaign, Urbana IL 61820

In this work we compute subleading oscillating terms in the Renyi entropy of Fermi gases and liquids corresponding to $2k_F$-like oscillations. Our theoretical tools are the one dimensional formulation of Fermi liquid entanglement familiar from discussions of the logarithmic violation of the area law and quantum Monte Carlo calculations. The main result is a formula for the oscillating term for any region geometry and a spherical Fermi surface in any dimension. Specializing to two dimensions, we compare this term to numerical calculations of Renyi entropies using the correlation function method and find excellent agreement. We also compare with quantum Monte Carlo data on interacting Fermi liquids where we also find agreement up to moderate interaction strengths.

I. INTRODUCTION

Fermi liquids are an extremely common form of quantum matter that appear in a wide range of physical systems including alkali metals, overdoped cuprate superconductors, and high density quark matter (before color superconductivity sets in). Cousins of the Fermi liquid have been observed in the half filled Landau level [1] and at a phenomenological level in layered organic salts [2]. The ubiquitous Fermi liquid has also played an important role in the recent exchange of ideas between quantum many-body physics and quantum information science. This exchange has resulted in a deeper appreciation of the important role of entanglement, especially long-range entanglement, in the physics of quantum matter like Fermi liquids. Long-range entanglement is important because it distinguishes interesting gapless phases like Fermi liquids and interesting gapped topological phases like fractional quantum Hall liquids from other more conventional phases like symmetry broken states that support long-range classical correlation but not long-range entanglement.

Much of the discussion about entanglement has turned on a quantity known as the entanglement entropy. We consider a large quantum system AB divided into two components A and B (typically A and B are spatial regions, but other "entanglement cuts" are possible). The entanglement entropy is then the von Neumann entropy $S(A) = -\mathrm{tr}_A(\rho_A \ln(\rho_A))$ of the state of A where $\rho_A = \mathrm{tr}_B(\rho_{AB})$. When the state of the whole system, ρ_{AB}, is pure, the von Neumann entropy $S(A)$ measures the amount of entanglement between A and B. We are especially interested in the case when $\rho_{AB} = |G\rangle\langle G|$ with $|G\rangle$ the ground state of a local Hamiltonian. It has also been profitable to consider the Renyi entropy,

$$S_n(A) = \frac{1}{1-n} \ln(\mathrm{tr}(\rho_A^n)), \tag{1.1}$$

which is actually a family of entropies labeled by n and which gives complete information about the spectrum of ρ_A, the "entanglement spectrum".

The basic rule governing the entanglement entropy in local ground states is the area law (for a review see Ref. [3]). For a system with short-ranged interactions in d spatial dimensions, the area law states that the entanglement entropy of a region A of linear size L grows like L^{d-1}, that is like the area $|\partial A|$ of the boundary ∂A of A. Fermi liquids are extremely interesting from an entanglement perspective because they possesses long-range entanglement that manifests as a violation of the area law [4–12]. Indeed, entanglement entropy in a Fermi liquid ground state scales like $L^{d-1}\ln(L)$ hence showing a logarithmic violation of the area law. Gapless systems in one dimension, including Luttinger liquids and quantum critical points, also show a logarithmic violation of the area law [13, 14], while most other gapped and gapless systems in $d > 1$ dimensions obey the area law. In fact, the logarithmic violations of the area law in $d = 1$ gapless theories and Fermi liquids are intimately related as we review below [6].

Another important development in the study of many-body entanglement has been the appearance of numerical studies of entanglement in a wide variety of systems. Entanglement in one dimension has long been accessible using DMRG (for a review see Ref. [15]), and free fermions and bosons are accessible via the correlation matrix method [16]. More recently, quantum Monte Carlo and tensor network calculations have permitted computations of entanglement in simple quantum magnets [17], more complex spin liquid states[18], topological states [19], and Fermi liquids [20]. We are thus finally in a position to begin a substantive comparison between theory and (numerical) experiment for universal terms in the entanglement entropy. We now have agreement between theory and experiment in one dimension, for certain simple topological phases in two dimensions, and for some symmetry broken states [21]. Various other predictions have been validated at a more qualitative level, including a prediction of $L\ln(L)$ entropy in a spin liquid with spinon Fermi surface [6, 18] and an observation of corner terms and terms associated with symmetry breaking in quantum magnets (although the agreement

here is not yet precise) [22, 23]. Very recently the first calculations of Renyi entropy in interacting Fermi liquids were reported in Ref. [20], with agreement at a quantitative level with previous theoretical predictions in Refs. [7, 24] up to intermediate interaction strength. Although it should be noted that discrepancies between these calculations and the theoretical predictions increase in the low density limit of the Fermi liquid, this represents one of the first examples in more than one dimension of precise quantitative agreement between theoretical and numerical computations of entanglement entropy in an interacting gapless system.

Previous work has focused on the leading logarithmic term in the Fermi liquid which was argued to depend only on the geometry of the interacting Fermi surface and on the geometry of A. However, as may be expected on general grounds and as was evident in the data in Ref. [20] and elsewhere, there are also subleading oscillating terms in the Renyi entropy. Similar oscillations have been extensively studied in one dimension [25–31]. Here we compute these subleading oscillating terms in the Renyi entropy analytically for the free Fermi gas in higher dimensions. We also argue that the period of oscillation and exponent of the power law prefactor are unmodified by interactions thus extending our results to Fermi liquids. Most of our arguments are carried out in two dimensions for concreteness, but we also record the general formulas in any dimension. We compare our results with extensive numerical data on free fermions and weakly interacting Fermi liquids in two dimensions and find agreement up to moderate interaction strengths. Thus we establish in considerable detail a quantitative agreement between theory and numerics regarding entanglement in weakly interacting Fermi liquids, both for the leading logarithmic violation as well as for the subleading oscillating term.

This paper is organized as follows. We first review the one dimensional aspects of Fermi liquid entanglement before deriving the form of the oscillating term in higher dimensions. We give an alternate proof for our formula when the region geometry is a long strip and further elucidate the structure of the entanglement spectrum in this case. Finally, we compare our theoretical predictions to numerical data for free and interacting Fermi liquids and find excellent agreement.

II. ENTANGLEMENT AND THE FERMI SURFACE

We now describe the theoretical framework for our calculations. Let R be the spatial region of interest in a Fermi liquid at zero temperature and let Γ denote the interacting Fermi sea. Once again, the Renyi entropy of region R is defined as

$$S_n(R) = \frac{1}{1-n} \ln \left(\mathrm{tr}(\rho_R^n) \right). \tag{2.1}$$

It is well known that the leading behavior of the Renyi entropy is $S_n \sim L^{d-1} \ln L$ where d is the spatial dimension and L is the linear size of R [4–8]. Furthermore, the Widom formula,

$$S_n \sim \left(1 + \frac{1}{n}\right) \frac{1}{24} \int_{\partial R} \frac{1}{(2\pi)^{d-1}} \int_{\partial \Gamma} |n_x \cdot n_k| \ln(L), \tag{2.2}$$

provides a precise characterization of the prefactor of the logarithmic term in terms of the geometry of the interacting Fermi surface $\partial\Gamma$ [5–7]. n_x and n_k are unit normals and the precise choice of length in the logarithm only modifies non-universal area law terms going like L^{d-1}.

This formula can be obtained by describing the Fermi surface as an infinite collection of one dimensional modes [6]. Each such one dimensional mode is a gapless chiral fermion which contributes to the entanglement entropy like $\frac{\ln(\ell)}{6}$ where ℓ is some effective length (see below). Adding up these contributions for each point on the real space boundary ∂R and each mode on the Fermi surface $\partial\Gamma$ leads to the Widom formula above. Even the dependence on the Renyi parameter n is predicted by the theory since the Renyi entropy of a single interval in a CFT is $\frac{n+1}{2n} \frac{\ln(\ell)}{6}$ [32]. Note also that each mode experiences many different effective lengths corresponding to different one dimensional cuts through the real space region, but to logarithmic accuracy we may replace all such lengths with any particular representative of the linear dimension L.

A. Oscillations in $d = 1$

It is also known that the Renyi entropy has a subleading oscillating term in one dimensional Luttinger liquids. This term is analogous to Friedel oscillations and hence occurs at momentum $2k_F$ [33]. For free fermions this term has the form

$$S_n^{d=1} \sim f_n \frac{\cos(2k_F \ell)}{(2k_F \ell)^{\beta_n}} \tag{2.3}$$

with $\beta_n = 2/n$ and

$$f_n = \frac{2}{1-n} \left(\frac{\Gamma((1+n^{-1})/2)}{\Gamma((1-n^{-1})/2)} \right)^2 \tag{2.4}$$

($\Gamma(z)$ is here the gamma function) [33]. Below we will use our one dimensional formulation of higher dimensional Fermi liquid entanglement to demonstrate the existence of similar oscillating terms in the entanglement entropy in higher dimensions.

First, however, we give a quick derivation of the 1d result using conformal field theory. The 1d electron operator may be decomposed as $c(x) = c_L(x) e^{-ik_F x} + c_R(x) e^{ik_F x}$ where $c_{L/R}$ are the left-moving and right-moving halves of a free relativistic fermion. They are the slowing varying fields entering the low energy description which we can use to compute universal terms in the entanglement entropy. The typical way we proceed is to introduce twist fields or otherwise study the system on an n-sheeted surface to compute $\mathrm{tr}(\rho^n)$. Here we simply note that an important feature of this setup is that translation symmetry is broken for $n \neq 1$. Furthermore, the singular branch points can in general produce localized relevant perturbations bound to them. These perturbations produce corrections to the leading CFT scaling of Renyi entropy (there are also bulk irrelevant operators that contribute) since they change the free energy in the branched background. This

perspective has been discussed in general in Ref. [34]; here we obtain identical results for the restricted case of interest to us.

For example, the action is perturbed to $\mathcal{S} = \mathcal{S}_{CFT} + g\phi(z_1) + g\phi(z_2)$ where $z_{1,2}$ are two branch points. The path integral is

$$Z = e^{-F} = \int D(\text{fields}) e^{-\mathcal{S}[\text{fields}]}$$
$$= Z_{CFT}(1 - g\langle(\phi(z_1) + \phi(z_2))\rangle +$$
$$\frac{g^2}{2}\langle(\phi(z_1) + \phi(z_2))^2\rangle + ...). \tag{2.5}$$

Note that we have not been careful about the n dependence in this schematic expression. Since $\langle\phi\rangle = 0$ the first correction to the free energy (upon re-exponentiating the series and with the usual story about disconnected diagrams) is of order g^2 and is essentially a correlator of the form $\langle\phi(z_1)\phi(z_2)\rangle$. To be specific, this is the part which depends on the separation of the branch points. We now go through this calculation in more detail for two branch points.

Consider a finite interval of length ℓ in the free fermion CFT. To produce an n-branched surface with branch points at z_1 and z_2 with $z_1 - z_2 = \ell$, we can consider the conformal transformation given by

$$w = \left(\frac{z - z_1}{z - z_2}\right)^{1/n} \tag{2.6}$$

where w is a coordinate on a plane while z is the branched coordinate. Indeed, we see that winding z around z_1 or z_2 winds w by a phase of $2\pi/n$, and hence we must wind z by $2\pi n$ to wind w by 2π. We now wish to compute correlations of operators inserted at z_1 and z_2 (the induced defect operators) to find corrections to the entropy. Given a primary field ϕ of dimension Δ we wish to find

$$\langle\phi(z)\phi(z')\rangle = \left|\frac{dw}{dz}\right|^{\Delta}\left|\frac{dw}{dz}\right|^{\Delta}\langle\phi(w)\phi(w')\rangle \tag{2.7}$$

where the equality follows from conformal invariance under the transformation in Eq. 2.6.

This equation is valid for all z and z' but we specifically want $z = z_1 + \epsilon$ and $z' = z_2 + \epsilon$ with ϵ a UV regulator. Assuming $\ell \gg \epsilon$ we obtain the following formulas:

$$\frac{dw}{dz} = \frac{1}{n}\left(\frac{\epsilon}{\ell}\right)^{1/n}\frac{1}{\epsilon}, \tag{2.8}$$

$$\frac{dw'}{dz'} = \frac{1}{n}\left(\frac{\ell}{\epsilon}\right)^{1/n}\frac{-1}{\epsilon}, \tag{2.9}$$

and

$$\langle\phi(w)\phi(w')\rangle = \frac{1}{|w - w'|^{2\Delta}} = \left(\frac{\epsilon}{\ell}\right)^{2\Delta/n}. \tag{2.10}$$

Putting everything together we find

$$\langle\phi(z_1)\phi(z_2)\rangle = \frac{1}{(n\epsilon)^{2\Delta}}\left(\frac{\epsilon}{\ell}\right)^{2\Delta/n} \tag{2.11}$$

which explicitly shows a correction of the form $\ell^{-2\Delta/n}$. Finally, to make contact with the Fermi gas result we must identify the relevant operator, but this operator is just the $2k_F$ density operator given by $e^{2ik_F x}c_L^\dagger(x)c_R(x)$ coming from the expansion of $c^\dagger(x)c(x)$. This operator has dimension $\Delta = 1$ and has an oscillating phase that is explicitly displayed. Thus the oscillating term in the entanglement entropy is indeed interpretable as a kind of $2k_F$ density response, albeit in a branched space (which accounts for the strange scaling dimension). Obtaining the prefactor for a given model requires more work since the field theory gives a cutoff dependent answer for the prefactor (which is anyway non-universal), but see Ref. [33] for a calculation for free fermions.

B. Oscillations in $d > 1$

We now return to the extension to higher dimensions. For concreteness, we set $d = 2$ and take R to a disk of radius L and Γ to be a disk of radius k_F. The extension of our results to arbitrary region shape (the analog of the Widom formula) is completely straightforward and will be recorded later. First, we must be more careful about the effective length ℓ since we are studying subleading terms. The appropriate choice is $\ell = \ell(x,k) = 2L|\cos\theta|$, where θ is the angle between n_x and n_k, which is nothing but the chordal distance across the circle (parallel to n_k) at angle θ [7, 8]. This choice is the effective one dimensional distance experienced by a mode propagating in the n_k direction starting at angle θ on the circle and reproduces the correct thermal entropy to entanglement entropy crossover function [7, 8].

The subleading oscillating term is then given by

$$f_n\frac{1}{2\pi}\frac{1}{4}\int_{\partial R}\int_{\partial\Gamma}|n_x \cdot n_k|\frac{\cos\left(2k_F\ell(x,k)\right)}{(2k_F\ell(x,k))^{\beta_n}}. \tag{2.12}$$

Plugging in our various expressions we find

$$S_n \sim f_n\frac{4k_FL}{8}\frac{1}{(4k_FL)^{2/n}}$$
$$\times\int_{-\pi/2}^{\pi/2}d\theta(\cos\theta)^{1-2/n}\cos\left(4k_FL\cos\theta\right). \tag{2.13}$$

The final integral may be simplified when $4k_FL$ is large since the integrand is rapidly oscillating. Focusing on the part of the integral near $\theta = 0$ we may write

$$\int d\theta e^{iu\cos\theta} \sim \int d\theta e^{iu(1-\theta^2/2)} \sim \sqrt{\frac{2\pi}{u}}e^{iu+i\phi} \tag{2.14}$$

where $\phi = \pm\pi/4$ is an unimportant phase. Note that this leading estimate is completely independent of n as regards

the integral over θ. Using this formula in our main expression gives, for $4k_F L$ large, the result

$$S_n \sim \frac{\sqrt{2\pi} f_n}{8} (4k_F L)^{1/2-2/n} \cos(4k_F L + \phi') \qquad (2.15)$$

where ϕ' is another phase. Thus we have a prediction for the prefactor, power lay decay, and period of oscillation of the oscillating term in the Renyi entropy for a free Fermi gas.

To complete this section we record the result for spherical Fermi surface and spherical real space region in general dimension d. The derivation is exactly as above in that we integrate the one dimensional result over the entire Fermi surface being careful the choose the correct effective length. This length is still simply $\ell = \ell(x,k) = 2L|\cos\theta|$, where θ is the angle between n_x and n_k (now in d dimensions). The general formula is then

$$\delta S_n = f_n \frac{1}{(2\pi)^{d-1}} \frac{1}{4} \int_{\partial R} \int_{\partial \Gamma} |n_x \cdot n_k| \frac{\cos(2k_F \ell(x,k))}{(2k_F \ell(x,k))^{\beta_n}} \qquad (2.16)$$

with ∂R and $\partial \Gamma$ now $d-1$ dimensional spheres of radii L and k_F respectively. Later we will generalize this result to arbitrary spatial region geometry.

III. INTERACTIONS

In this section we discuss the role interactions in our results, but we will only consider $d = 2$ for simplicity. The interacting fixed point theory is Landau's Fermi liquid theory which is characterized by an infinite set of forward scattering interactions labelled by Landau parameters. Because the only interactions that survive in the low energy limit are forward scattering terms, the low energy theory has a large emergent symmetry group conventionally denoted $U(1)^\infty$. What is meant by this expression is that forward scattering interactions preserve the number of quasiparticles at each point on the Fermi surface. In other words, in the scattering process $(k_1^i, k_2^i) \to (k_1^f, k_2^f)$ we always have $(k_1^i, k_2^i) = (k_1^f, k_2^f)$ or $(k_1^i, k_2^i) = (k_2^f, k_1^f)$.

Since the low energy theory still has a sharp Fermi surface and since the number of quasiparticles at each point on the Fermi surface is conserved at low energies, the low energy theory is almost free. In particular, the non-zero quasiparticle residue implies that the system has a large number of extended states which are physically similar to free fermionic plane waves (non-zero overlap) and which are exact eigenstates of the interacting Hamiltonian (quasiparticle decay rate vanishes at the Fermi surface). This is the basic intuition behind the claim that even Fermi liquids will have $L \ln(L)$ entanglement entropy given by the Widom formula evaluated for the true interacting Fermi surface.

Now turning to the sub-leading oscillations, we expect that when interactions are turned the emergent $U(1)^\infty$ symmetry will protect the exponent of the power law, but the numerical prefactor may be modified [7, 8]. For example, in one dimension the prefactor depends on the Luttinger parameter [33], but while the power law decay is also modified in one dimension, in higher dimensions the power law should remain unchanged since quasiparticles remain sharp. The momentum of the oscillation will remain at the interacting $2k_F$, that is, while interactions may change the non-interacting Fermi surface, the correct momentum is always $2k_F$ for the physical Fermi surface.

Physically these expectations are based on the following argument. As argued in Section II, the subleading oscillating terms come from insertions of relevant operators bound to the branch points (in $d = 1$) or branch lines (in $d = 2$). Indeed, in the one dimensional case we identified the important operator as the $2k_F$ density operator. Thus for the purposes of computing subleading oscillating terms in a Fermi liquid we must study correlators of $2k_F$ density operators in a branched space. Since Fermi liquids have $2k_F$ oscillations at the interacting $2k_F$ with the same power law decay as in a Fermi gas but with a non-universal prefactor, our claims above are justified.

There is a simple exactly solvable model in which these claims can be checked. We study Landau's Hamiltonian for the Fermi liquid which takes the form

$$H_{FL} = \sum_k (\epsilon_k - \mu) n_k + \frac{1}{2} \sum_{kk'} f_{kk'} n_k n_{k'}. \qquad (3.1)$$

The $U(1)^\infty$ symmetry refers to the fact that $[H_{FL}, n_k] = 0$ for all k and hence H_{FL} has an infinite number of conserved quantities. Indeed, the ground state of this interacting Hamiltonian is a free fermion wavefunction with a Fermi sea Γ obtained by solving the self consistent equations

$$\tilde{\epsilon}_k \leq 0, k \in \Gamma \qquad (3.2)$$

and

$$\tilde{\epsilon}(k) = \epsilon_k - \mu + \sum_{k' \in \Gamma} f_{kk'}. \qquad (3.3)$$

For example, if we work in a rotationally invariant system and impose Luttinger's theorem (by adjusting the chemical potential) then the interacting Fermi surface always coincides with the free surface which is in turn determined solely by the density.

More generally, although the Fermi surface can change as interactions are tuned (e.g. in a lattice model with non-spherical Fermi surface), the entanglement entropy always obeys the Widom formula evaluated on the physical interacting Fermi surface. Similarly, all subleading corrections to the entropy in the toy model in Eq. 3.1 are those of a Fermi gas with Fermi surface $\partial\Gamma$. However, we emphasize that this is not necessarily the correct answer for a physical Fermi liquid since the pure forward scattering model in Eq. 3.1 requires long-range interactions and hence is not in the same universality class as a short-ranged Fermi liquid. This is reflected physically in the fact that while Eq. 3.1 has an exact $U(1)^\infty$ symmetry, the same symmetry in a short-ranged Fermi liquid is only emergent at low energies.

Our argument for universality has also recently been explicitly validated in Ref. [35]. That work examined a model of a

Fermi liquid in which the quasiparticle residue could be continuously tuned to zero at a quantum critical point, but where density and current correlation functions were those of a free Fermi gas. In the language of Fermi liquid theory, the Landau parameters have been tuned to zero, but the quasiparticle residue is non-trivial. Nevertheless, the system is a non-trivial interacting Fermi liquid and Ref. [35] showed that the Widom formula for the leading logarithmic violation is still exactly obeyed. Furthermore, the oscillating terms we considered here are also present, unmodified, in the particular realization of an interacting Fermi liquid in Ref. [35]. This suggests that the prefactor of the oscillating term can be expected to be near the free result provided the Landau parameters are small even if the quasiparticle residue is tiny.

IV. OSCILLATIONS FOR GENERAL SPATIAL REGIONS IN $d > 1$

Now we turn to the general formula for the subleading oscillating term in the Renyi entropy of a free Fermi gas for a convex but otherwise arbitrary region shape. Let us first discuss the case of $d = 2$. Again, R is the real space region of linear size L and Γ is the spherical Fermi sea. We can also generalize to more complex Fermi seas in a straightforward way. Let x and k denote points on ∂R and $\partial\Gamma$ respectively, and define the effective length $\ell(x,k)$ to be the length of the line segment given by the intersection of the line $\{x + n_k s | s \in (-\infty, \infty)\}$ and R. The convexity of R guarantees that this intersection is a single line segment. It can also be checked that this definition reduces to our prescription for ℓ for a spherical region R given above. The subleading correction to the Renyi entropy is then

$$S_n \sim \frac{f_n}{2\pi}\frac{1}{4}\int_{\partial R}\int_{\partial\Gamma} |n_x \cdot n_k| \frac{\cos\left(2k_F \ell(x,k)\right)}{(2k_F\ell(x,k))^{2/n}}. \tag{4.1}$$

In general dimension d, the definition of the effective length is exactly as above. Convexity of R still guarantees that the effective length is well defined and corresponds to a single interval, that is a straight connected one dimensional subset of R. The general expression is then

$$\delta S_n = f_n \frac{1}{(2\pi)^{d-1}}\frac{1}{4}\int_{\partial R}\int_{\partial\Gamma} |n_x \cdot n_k| \frac{\cos\left(2k_F \ell(x,k)\right)}{(2k_F\ell(x,k))^{\beta_n}} \tag{4.2}$$

with ∂R and $\partial\Gamma$ now $d-1$ dimensional spaces ($\partial\Gamma$ is still a sphere).

A. Strip geometry in $d = 2$

We have already applied this formula to case when R is a disk. It is also enlightening to consider a long strip region. Thus suppose the region R is a long strip of length L and width W with $L \gg W$, and let θ be the angle between the Fermi surface normal and real space normal. The effective distance is found to be $\ell = W/|\cos\theta|$ so long as $\ell \ll L$ which we take to be essentially infinite. Alternatively, we can consider a strip that wraps completely around the cycle of a torus of length L in which case translation invariance in the L direction is manifestly preserved. Within our approximation we find

$$S_n \sim \frac{f_n k_F L}{2\pi}\int_{-\pi/2}^{\pi/2} d\theta \cos\theta \left(\frac{\cos\theta}{2k_F W}\right)^{2/n} \cos\left(\frac{2k_F W}{\cos\theta}\right). \tag{4.3}$$

Assuming $2k_F W \gg 1$ we may perform the θ integral as above by focusing on the region near $\theta = 0$. The result is

$$S_n \sim \frac{f_n k_F L}{2\pi}\left(\frac{1}{2k_F W}\right)^{2/n}\sqrt{\frac{2\pi}{2k_F W}}\cos\left(2k_F W\right). \tag{4.4}$$

Part of the reason why the strip case is interesting is that we may obtain the above result in another way. We can also say a great deal about the entanglement spectrum of the strip. The results are, however, restricted to free theories only. Thus consider again a free Fermi gas with spherical Fermi surface and examine the fermion two-point function $G(r-s) = \langle c^\dagger(r)c(s)\rangle$. This function may be obtained from a Fourier transform of the occupation number n_k as

$$G = \int \frac{d^2k}{(2\pi)^2} n_k e^{ik\cdot(r-s)} \tag{4.5}$$

where $n_k = \theta(k_F - |k|)$. Our interest in this function is that, by virtue of Wick's theorem, it completely determines the reduced density matrix of a region R provided we restrict $r, s \in R$. This is the standard correlation matrix method (see the appendix).

Let $\hat{K}$ be the entanglement Hamiltonian ($\rho = e^{-\hat{K}}$) for the infinite strip (length L, see above). We know that $\hat{K}$ has the form

$$\hat{K} = \sum_{r,s\in R} K(r,s) c^\dagger(r) c(s) \tag{4.6}$$

because of Wick's theorem. Furthermore, the "matrix" K is related to G via $G = \frac{1}{e^K+1}$ (proven by diagonalizing the "matrix" G with r, s restricted to R). Translation invariance in the L direction enables us to write

$$K = K(r_W, s_W, r_L, s_L) = K(r_W, s_W, r_L - s_L, 0) \tag{4.7}$$

where the subscript indicates the L or W directions. Upon Fourier transforming over $r_L - s_L$ this becomes,

$$\hat{K} = \sum_{0\le r_W, s_W \le W, k} K_{1d}(r_W, s_W, k) c^\dagger(r_W, k) c(s_W, k). \tag{4.8}$$

The new matrix K_{1d} is related to the partial Fourier transform G. Consider the mixed position/momentum basis function

$$\begin{aligned} G_{1d}(r_W - s_W, k) &= \sum_{r_L} G(r_W - s_W, r_L) e^{-ikr_L} \\ &= \int_{-\sqrt{k_F^2-k^2}}^{\sqrt{k_F^2-k^2}} \frac{dq}{2\pi}\theta(k_F - \sqrt{q^2+k^2}) e^{iq(r_W - s_W)} \end{aligned} \tag{4.9}$$

which is nothing but the two-point function of a *one dimensional* Fermi gas with Fermi momentum $k_F^{1d}(k) = \sqrt{k_F^2 - k^2}$. Because both K and G are partially diagonalized by the Fourier transformation in the 2 direction we immediately have that

$$G_{1d}(k) = \frac{1}{e^{K_{1d}(k)} + 1}. \tag{4.10}$$

Thus K_{1d} is the single particle entanglement Hamiltonian for a one dimensional Fermi gas of Fermi momentum $k_F^{1d} = \sqrt{k_F^2 - k^2}$ on an interval of length W. The full entanglement spectrum of the two dimensional strip is also now known in terms of the one dimensional spectrum e.g. we have a complete one dimensional spectrum for an interval of length W for each value of $k \in [-k_F, k_F]$. Of course, this result is trivially generalizable to strips in general d using translation invariant along the $d-1$ long directions of the strip.

Using this information we can immediately check the leading $L \log(W)$ term in the entropy. The entropy from each value of k is $\ln(W)/3$ and hence the total entropy is (to leading order)

$$S = L \int_{-k_F}^{k_F} \frac{dk}{2\pi} \frac{\log(W)}{3} = \frac{k_F L}{3\pi} \ln(W). \tag{4.11}$$

A quick calculation with the Widom formula gives

$$\begin{aligned} S &= \frac{1}{12} \frac{1}{2\pi} (2\pi L)(2k_F) \int_{-\pi/2}^{\pi/2} d\theta \cos\theta \ln(W) \\ &= \frac{k_F L}{3\pi} \ln(W). \end{aligned} \tag{4.12}$$

Returning now to the oscillating term, we can use Eq. 2.3 to estimate the oscillating term for the strip in a different way. Each one dimensional spectrum identified above will contribute an oscillating term but with a variable k_F^{1d}. The oscillating term is thus

$$S_n \sim f_n L \int_{-k_F}^{k_F} \frac{dk}{2\pi} \frac{\cos(2\sqrt{k_F^2 - k^2} W)}{(2\sqrt{k_F^2 - k^2} W)^{\beta_n}}. \tag{4.13}$$

As we have now repeatedly observed, if $k_F W$ is large then the integrand is rapidly oscillating and the integral is dominated by values of k near zero. Performing the effective Gaussian integral over k we find

$$S_n \sim \frac{f_n L}{2\pi} \sqrt{\frac{\pi k_F}{W}} \frac{\cos(2k_F W)}{(2k_F W)^{2/n}} \tag{4.14}$$

or

$$S_n \sim \frac{f_n k_F L}{2\pi} \sqrt{\frac{2\pi}{2k_F W}} \frac{\cos(2k_F W)}{(2k_F W)^{2/n}} \tag{4.15}$$

which is identical to our previous result. Note how the two methods obtain the same final form by integrating over either an effective length or an effective Fermi momentum.

V. COMPARISON BETWEEN THEORY AND NUMERICS IN $d = 2$

We will now compare our theoretical predictions with numerical data for the Renyi entropy of the free Fermi gas for two subsystem geometries, strips and circles, in $d = 2$. The total system is a torus with periodic boundary conditions. All numerical data was produced using the correlation function technique extended to continuum Hamiltonians [16, 36, 37]. We emphasize that all the systems we consider are continuum models with rotational invariant, there is no spatial lattice. The numerical procedure relies on the discretization of momentum space which is then converged with respect to grid density. Fits to the data were performed using a standard nonlinear least squares (NLLS) package excluding data from very small regions [16, 36–38]. Computational details for computing Renyi entropies can be found in Appendix A.

Our fitting strategy is two-fold, first we fit the Renyi entropy to our scaling form and allow all parameters to vary, then we perform a second fit with fixed values for the theoretical parameters our analysis provides. Fit procedure one is a challenging test for the theory and for the numerics because of the sensitivity of the fit for a finite range of data. For small region size, L, it may be difficult to differentiate between L and a $L\log(L)$ scaling laws. We expect for these terms, L and $L\log(L)$, to match the theoretical values as we reach very large region size. By performing this first fitting procedure we show that the system sizes we have investigated are sufficiently large to reach the asymptotic scaling regime. The second fitting procedure allows us to test how well the theory can describe the numerical data, and provide estimates for the unknown parameters. The parameters from fit procedure one are denoted as a_i^{fit}, for fit procedure two they will be denoted $\tilde{a}_i^{\text{fit}}$, and analytical values of the parameters will be denoted, a_i^{theory}.

A. Circular geometry

For the circular geometry, we work in units where $k_F = 2$ so that the density of a spin polarized gas is $n = k_F^2/(4\pi) = 1/\pi$. This implies that the average number of particles in the real space circle is $\langle N \rangle = \pi L^2 n = L^2$. In the figure we show Renyi entropies of a free Fermi gas computed numerically for disks with up to $L = 15$. The numerical data is fit to the following functional form

$$S_n(L) = a_1 L \ln(L) + a_2 L + a_3 \frac{\cos(a_4 L + a_5)}{L^{a_6}}, \tag{5.1}$$

Four of these parameters have values predicted by theory:

$$a_1 = \frac{n+1}{3n} \tag{5.2}$$

(from the Widom fomula),

$$|a_3| = |f_n| \frac{\sqrt{2\pi}}{8^{1/2+2/n}} \tag{5.3}$$

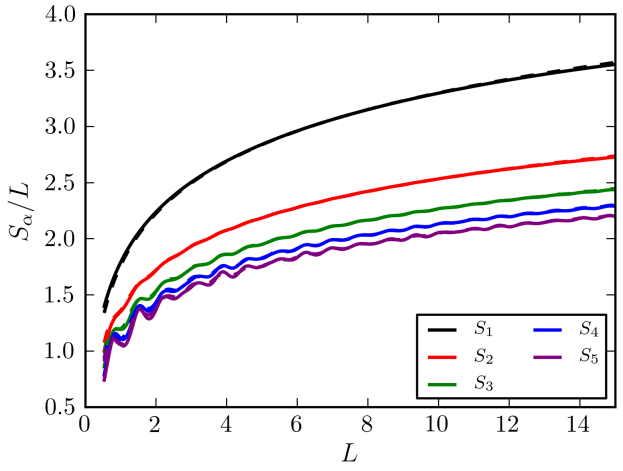

FIG. 1. Renyi entropies S_1 through S_5 divided by length, L, for the circular geometry. Solid lines are data and dashed lines are with theoretical values for the parameters in equation 5.1 found on the left side of table I and $\tilde{a}_2^{\text{fit}}$ and $\tilde{a}_5^{\text{fit}}$ from Table II.

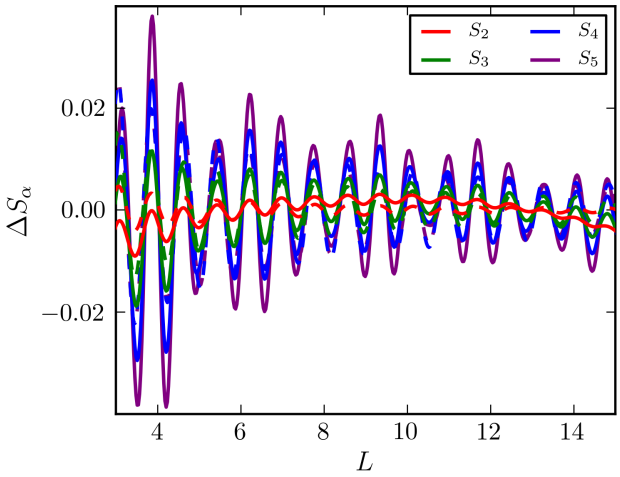

FIG. 2. We remove the leading scaling term by subtracting the fit L and $L\log L$ terms from the data for the circular region and plot against our theoretical predictions. The frequency of the oscillations for numerics and theory is in excellent agreement. The magnitude of the oscillations is slightly underestimated for small regions, and is increasingly underestimated as the Renyi parameter α is increased. For large α Renyi entropy a second oscillation frequency is apparent. There also exists a smaller subleading scaling correction which can be seen most clearly in the slight downward curvature of ΔS_2.

$$a_6 = \frac{2}{n} - \frac{1}{2} \tag{5.4}$$

and $a_4 = 4k_F$. The parameters a_2 and a_5 are not predicted by our theory and are determined by fitting the numerical data. This form of the scaling law includes our new prediction for the subleading oscillations as well as the leading order term from the Widom conjecture and the area law term.

In Table I we provide the parameters determined by our analysis as well as those from fit procedure one. We note the excellent agreement between $\{a_i^{\text{theory}}\}$ and $\{a_i^{\text{fit}}\}$. There is some trade-off between a_1^{fit} and a_2^{fit} for the finite fitting range. When fitting procedure two is performed, and all known parameters are fixed at their theoretical values, $\tilde{a}_2^{\text{fit}}$ is decreased. The results for the second fitting procedure are found in table II and plotted in figure 1. Again, the quality of the agreement is remarkable, the numerical data and fit are indistinguishable at all but the smallest of L.

To illustrate more clearly the agreement between theory and numerics we remove the leading scaling term and plot the remainder in figure 2. For this region geometry the oscillation frequency for the numerics and theory agrees exactly. The magnitude of the oscillations is also in agreement though less so for small region size and the higher order Renyi entropies. The agreement between theory and numerics may be improved by more accurate calculation of the integral in equation 2.14.

Additional subleading terms contribute to a systematic deviation from the leading scaling law and oscillations which is most obvious for S_2 in figure 2. The prefactor for these additional terms are an order of magnitude smaller than the oscillating terms. As we will show, these corrections do not exist for the strip geometry and are likely due to the geometry of the spatial region.

B. Strip geometry

For the strip geometry we work with the same density as in the circular case. Here we parameterize our fitting function as,

$$S_n(W) = a_1 \ln(W) + a_2 + a_3 \frac{\cos(a_4 W + a_5)}{W^{a_6}}. \tag{5.5}$$

Our analysis predicts

$$a_1 = \frac{n+1}{3n}\frac{k_F L}{2\pi} \tag{5.6}$$

(from the Widom fomula),

$$a_3 = \frac{|f_n| L\sqrt{k_F}}{2\sqrt{\pi}(2k_F)^{2/n}} \tag{5.7}$$

$$a_6 = \frac{2}{n} + \frac{1}{2} \tag{5.8}$$

and $a_4 = 2k_F$.

The results for fitting procedure one for this geometry are provided in Table III. Because some of these parameters are explicitly dependent on the length of the system, we present results for a_1, a_2, and a_4 with the length scale removed. For the strip geometry the agreement between theory and numerics is equally impressive. As was the case for the circular geometry, we note the complimentary behavior of the two leading terms, $\log(L)$ and a constant in this case when performing fitting procedure two. Results for fitting procedure two can be found in table IV and are plotted in figure 3.

n	a_1^{theory}	a_3^{theory}	a_4^{theory}	a_6^{theory}
1	0.667			
2	0.500	0.0253	8	1/2
3	0.444	0.0566	8	1/6
4	$0.41\bar{6}$	0.0765	8	0
5	0.400	0.0869	8	-1/10

n	a_1^{fit}	a_2^{fit}	a_3^{fit}	a_4^{fit}	a_5^{fit}	a_6^{fit}
1	0.650	1.799				
2	0.493	1.395	0.0185	8.02	0.552	0.40
3	0.440	1.251	0.0533	8.02	0.559	0.17
4	0.413	1.176	0.0772	8.02	0.583	0.03
5	0.396	1.131	0.0912	8.01	0.600	-0.06

TABLE I. Comparison between (left) theory and (right) numerical data for the circular geometry. The parameterization is given by equation 5.1. The fit is performed with all parameters free to illustrate how well theory predicts the parameters. As the size of the system is increased the linear term, a_2, decreases and a_1 increases. For small system sizes L and $L\log(L)$ have a large overlap.

n	$\tilde{a}_2^{\text{fit}}/L$	$\tilde{a}_5^{\text{fit}}$
1	1.77	
2	1.38	0.632
3	1.24	0.690
4	1.17	0.707
5	1.13	0.715

TABLE II. Fit parameters, $\tilde{a}$, for the circular geometry, equation 5.1, with all known theoretical values fixed. We denote these with a tilde to differentiate them from the fit values of table I which were obtain allowing all parameters to vary. With just these two degrees of freedom we are able to obtain excellent agreement between the numeric and theoretical Renyi entropies.

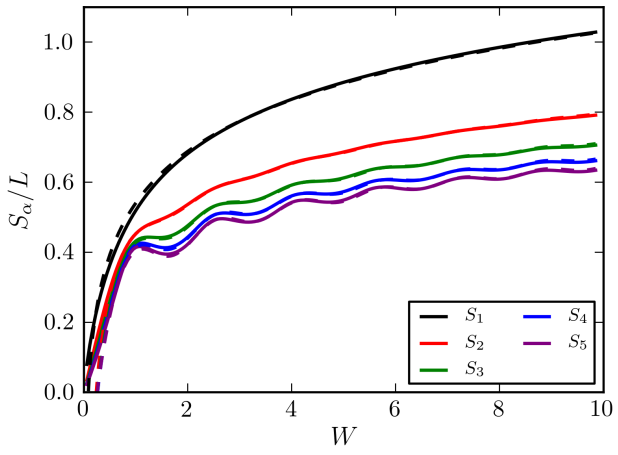

FIG. 3. Renyi entropies S_1 through S_5 for the strip geometry. Solid lines are data and dashed lines are with theoretical values for the parameters in equation 5.5 found on the left side of table III and $\tilde{a}_2^{\text{fit}}$ and $\tilde{a}_5^{\text{fit}}$ from Table IV.

As was the case for the circular geometry, we present in figure 4 the Renyi entropy S_2 through S_5 with the leading terms removed. In this case the oscillation frequency and magnitude are in excellent agreement. We also note the lack of additional subleading corrections.

C. Interactions

Finally, we briefly discuss how our arguments from Section III compare with interacting data from Ref. [20]. In

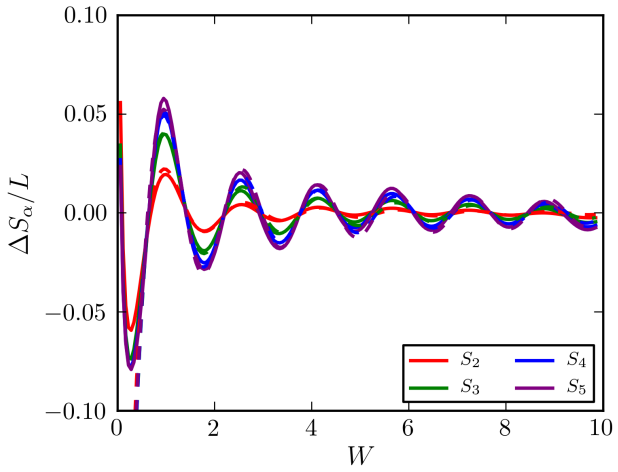

FIG. 4. We remove the leading scaling term by subtracting the fit constant and $\log L$ terms from the data for the cylindrical strip and plot against our theoretical predictions. The magnitude and frequency of the oscillations is almost identical for numerics and theory.

that work Renyi entropies were computed for various interacting Fermi liquids as a function of interaction strength for both short-range interactions and Coulomb interaction using the swap operator in quantum Monte Carlo [17]. The subleading oscillations in S_2 for the spin polarized electron gas and the free electron gas, shown in figure 5, agree well even for moderate interaction strength. This agreement may be improved further by computing larger region sizes in QMC for comparison. Though the range of the data is somewhat limited, this provides numerical evidence for our earlier theoretical claim that the period and power law prefactor of the decay is unchanged by weak interactions. Additionally, as we described above, Ref. [35] has shown that for a certain solvable model of an interacting Fermi liquid, the proposed universality of Renyi entropies is indeed exactly true.

However, let us also emphasize that preliminary data taken from Ref. [20] and plotted in figures 5 and 6, show that the oscillating terms may deviate from the free results in the limit of strong interactions and large Renyi parameter. Indeed, Ref. [20] already observed that even the $L\ln(L)$ term has a small but systematic growth with $r_s = \sqrt{\text{Area}/N_e\pi}$, the Wigner-Seitz radius, once $r_s \gg 1$ which is not predicted by the theory. The Wigner-Seitz radius is approximately proportional to the

n	a_1^{theory}/L	a_3^{theory}/L	a_4^{theory}	a_6^{theory}
1	0.212			
2	0.159	0.0228	4	3/2
3	0.141	0.0405	4	7/6
4	0.133	0.0487	4	1
5	0.127	0.0516	4	9/10

n	a_1^{fit}/L	a_2^{fit}/L	a_3^{fit}/L	a_4^{fit}	a_5^{fit}	a_6^{fit}
1	0.220	0.530				
2	0.157	0.434	0.0204	4.07	2.00	1.45
3	0.139	0.393	0.0390	4.05	2.10	1.19
4	0.130	0.371	0.0481	4.04	2.15	1.03
5	0.124	0.358	0.0527	4.04	2.18	0.95

TABLE III. Comparison between (left) theory and (right) numerical data for the strip geometry. We divide the length of the system out out of a_1, a_2, and a_3. The parameterization is given by equation 5.5.

n	$\tilde{a}_2^{\text{fit}}$	$\tilde{a}_5^{\text{fit}}$
1	0.542	
2	0.432	2.052
3	0.389	2.162
4	0.367	2.218
5	0.353	2.244

TABLE IV. Fit parameters, $\tilde{a}$, for the strip geometry, equation 5.5, with all known theoretical values fixed. We denote these with a tilde to differentiate them from the fit values of table III which were obtain allowing all parameters to vary. As was the case with the circular geometry, we obtain excellent agreement between numeric and theoretical Renyi entropy scaling laws.

ratio of potential to kinetic energy for the system and increases as inter-particle correlations increase. The origin of this dependence is not yet understood. For the oscillating terms, it seems that the wavevector is indeed consistent with our arguments above, but the prefactor may be modified. Thus while our arguments for interacting Fermi liquids have been vindicated by numerical data for moderate interaction strengths, the situation at strong coupling is more complex. Thus we defer a detailed analysis of that case to future work.

VI. CONCLUSIONS

In this paper we have considered subleading oscillating terms in the Renyi entropy of free Fermi gases and Fermi liquids. We gave a simple analytic formula for the subleading oscillating term using the one-dimensional formulation of Fermi liquid entanglement. This formula compares favorably with numerical calculations of the Renyi entropy of free Fermi gases in various geometries. We also considered the effects of weak interactions and argued for a certain degree of universality in the subleading oscillating term. Our arguments were checked by comparing to previous quantum Monte Carlo calculations of Renyi entropies in Fermi liquids as well as by comparing to exact results in a solvable model of a Fermi liquid. Thus we have established excellent agreement between theory and numerics for both the leading and subleading terms in the Renyi entropy of weakly interacting Fermi liquids.

An interesting future direction, which we have only just touched on here, is the exploration of the physics of the entanglement spectrum which plays an important role in topological systems [39–43]. We know the full spectrum for a

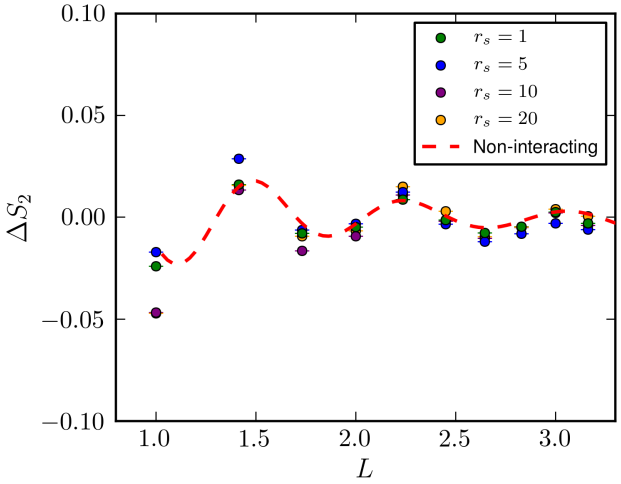

FIG. 5. Data from Ref. [20] for S_2 of the spin polarized electron gas across $r_s = 1, 5, 10, 20$, defined in the text, with leading scaling term removed. The dashed line is from the numerical analysis of the non-interacting system. The oscillation frequency for the interacting case is the same as the non-interacting case, though the magnitude of the oscillations may be modified.

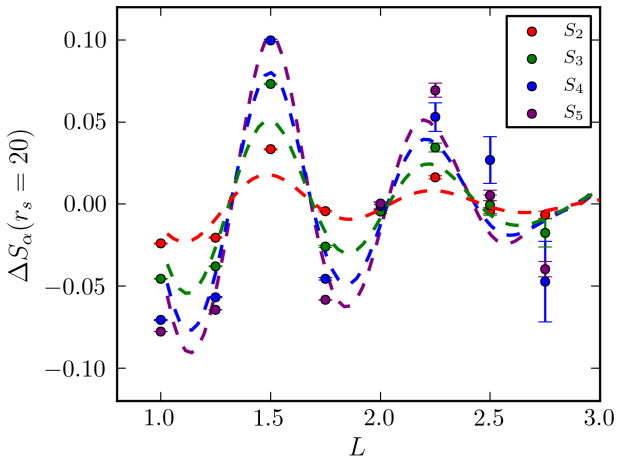

FIG. 6. Data from Ref. [20] for Renyi parameters 2, 3, and 4 for the spin polarized electron gas at $r_s = 20$, in the strongly interacting regime, with leading scaling term removed. The dashed lines are the computed subleading oscillation for each Renyi parameter from the preceeding numerical data. The error in the quantum Monte Carlo data grows quickly with region size and Renyi parameter. As shown in figure 5, the oscillation frequency appears unchanged by interactions though the magnitude may be increased.

strip, but more generally it would be desirable to have an understanding the spectrum of more general regions and in the presence of interactions. Something like the bulk-edge correspondence for topological phases should be valid for Fermi liquids as well, but the precise form of this correspondence remains uncertain. It would also be very interesting to extend our results to other kinds of quantum matter which support a Fermi surface but which may not be simple Fermi liquids. Entanglement entropy in these models provide a conceptually simple probe of the Fermi surface, even if it is not associated with conventional electrons, and since both the oscillating term and the leading logarithmic term know about the Fermi surface geometry, we can extract the universal prefactor (analogous to the central charge) in front of the logarithmic term in the Renyi entropy. Finally, although we considered only spherical Fermi surfaces here, it is possible to extend our results to more general Fermi surface shapes.

VII. ACKNOWLEDGEMENTS

JBM and NMT were supported by the National Science Foundation under grant OCI-0904572. This work was performed in part by JBM under the auspices of the US Department of Energy (DOE) by LLNL under Contract DE-AC52-07NA27344, document number LLNL-JRNL-635484. BGS is supported by a Simons Fellowship through Harvard University. This work used the Extreme Science and Engineering Discovery Environment (XSEDE), which is supported by National Science Foundation grant number OCI-1053575.

[1] B. I. Halperin, P. A. Lee, and N. Read, Phys. Rev. B **47**, 7312 (1993).
[2] M. Yamashita, N. Nakata, Y. Senshu, M. Nagata, H. M. Yamamoto, R. Kato, T. Shibauchi, and Y. Matsuda, Science **328**, 1246 (2010).
[3] J. Eisert, M. Cramer, and M. B. Plenio, Rev. Mod. Phys. **82**, 277 (2010).
[4] M. M. Wolf, Phys. Rev. Lett. **96**, 010404 (2006).
[5] D. Gioev and I. Klich, Phys. Rev. Lett. **96**, 100503 (2006).
[6] B. Swingle, Phys. Rev. Lett. **105**, 050502 (2010).
[7] B. Swingle, Phys. Rev. B **86**, 035116 (2012).
[8] B. Swingle, Phys. Rev. B **86**, 045109 (2012).
[9] W. Li, L. Ding, R. Yu, T. Roscilde, and S. Haas, Phys. Rev. B **74**, 073103 (2006), arXiv:quant-ph/0602094.
[10] S. Farkas and Z. Zimborás, Journal of Mathematical Physics **48**, 102110 (2007), arXiv:0706.1805 [math-ph].
[11] R. C. Helling, H. Leschke, and W. L. Spitzer, ArXiv e-prints (2009), arXiv:0906.4946 [math-ph].
[12] L. Ding, N. Bray-Ali, R. Yu, and S. Haas, Phys. Rev. Lett. **100**, 215701 (2008).
[13] C. Holzhey, F. Larsen, and F. Wilczek, Nuc. Phys. B **424**, 443 (1994).
[14] P. Calabrese and J. Cardy, J. Stat. Mech. **04**, 06002 (2004).
[15] U. Schollwöck, Rev. Mod. Phys. **77**, 259 (2005).
[16] I. Peschel, Journal of Physics A: Mathematical and General **36**, L205 (2003).
[17] M. B. Hastings, I. González, A. B. Kallin, and R. G. Melko, Phys. Rev. Lett. **104**, 157201 (2010).
[18] Y. Zhang, T. Grover, and A. Vishwanath, Physical Review Letters **107**, 067202 (2011), arXiv:1102.0350 [cond-mat.str-el].
[19] H.-C. Jiang, Z. Wang, and L. Balents, ArXiv e-prints (2012), arXiv:1205.4289 [cond-mat.str-el].
[20] J. McMinis and N. M. Tubman, ArXiv e-prints (2012), arXiv:1207.4188 [cond-mat.str-el].
[21] H. F. Song, N. Laflorencie, S. Rachel, and K. Le Hur, Phys. Rev. B **83**, 224410 (2011).
[22] A. B. Kallin, M. B. Hastings, R. G. Melko, and R. R. P. Singh, Phys. Rev. B **84**, 165134 (2011), arXiv:1107.2840 [cond-mat.str-el].
[23] M. A. Metlitski and T. Grover, ArXiv e-prints (2011), arXiv:1112.5166 [cond-mat.str-el].
[24] W. Ding, A. Seidel, and K. Yang, Phys. Rev. X **2**, 011012 (2012).
[25] E. S. Sørensen, M.-S. Chang, N. Laflorencie, and I. Affleck, Journal of Statistical Mechanics: Theory and Experiment **1**, 1 (2007), arXiv:cond-mat/0606705.
[26] P. Calabrese and F. H. L. Essler, Journal of Statistical Mechanics: Theory and Experiment **8**, 29 (2010), arXiv:1006.3420 [cond-mat.stat-mech].
[27] J. C. Xavier and F. C. Alcaraz, Phys. Rev. B **85**, 024418 (2012), arXiv:1111.6577 [cond-mat.stat-mech].
[28] M. Fagotti and P. Calabrese, Journal of Statistical Mechanics: Theory and Experiment **1**, 17 (2011), arXiv:1010.5796 [cond-mat.stat-mech].
[29] M. Dalmonte, E. Ercolessi, and L. Taddia, Phys. Rev. B **84**, 085110 (2011).
[30] P. Calabrese, M. Mintchev, and E. Vicari, Journal of Statistical Mechanics: Theory and Experiment **9**, 28 (2011), arXiv:1107.3985 [cond-mat.stat-mech].
[31] P. Calabrese, M. Mintchev, and E. Vicari, Physical Review Letters **107**, 020601 (2011), arXiv:1105.4756 [cond-mat.stat-mech].
[32] P. Calabrese and J. Cardy, Journal of Statistical Mechanics: Theory and Experiment **6**, 2 (2004), arXiv:hep-th/0405152.
[33] P. Calabrese, M. Campostrini, F. Essler, and B. Nienhuis, Phys. Rev. Lett. **104**, 095701 (2010).
[34] J. Cardy and P. Calabrese, Journal of Statistical Mechanics: Theory and Experiment **4**, 23 (2010), arXiv:1002.4353 [cond-mat.stat-mech].
[35] B. Swingle, ArXiv e-prints (2012), arXiv:1209.0769 [cond-mat.str-el].
[36] N. M. Tubman and J. McMinis, ArXiv e-prints (2012), arXiv:1204.4731 [cond-mat.str-el].
[37] P. Calabrese, M. Mintchev, and E. Vicari, EPL (Europhysics Letters) **97**, 20009 (2012).
[38] T. Williams and C. Kelley, "Gnuplot 4.6," `http://gnuplot.info/` (2012).
[39] H. Li and F. D. M. Haldane, Phys. Rev. Lett. **101**, 010504 (2008).
[40] X.-L. Qi, H. Katsura, and A. W. W. Ludwig, Physical Review Letters **108**, 196402 (2012), arXiv:1103.5437 [cond-mat.mes-hall].
[41] B. Swingle and T. Senthil, Phys. Rev. B **86**, 045117 (2012), arXiv:1109.1283 [cond-mat.str-el].
[42] A. M. Läuchli, E. J. Bergholtz, J. Suorsa, and M. Haque, Phys. Rev. Lett. **104**, 156404 (2010).

[43] I. Peschel and M.-C. Chung, EPL (Europhysics Letters) **96**, 50006 (2011), arXiv:1105.3917 [cond-mat.stat-mech].

Appendix A: Computational Details

We compute the Renyi entropies from the eigenvalues of a spatially reduced density matrix using an extension of the correlation function technique to continuum systems [16, 37]. For a free particle Hamiltonian,

$$\hat{H} = -\sum_{m,n} \hat{t}_{m,n} c_n^\dagger c_m \tag{A1}$$

with n and m subsystem site indices, and c_i and $c_i^\dagger$ the creation and annihilation operators for state i, eigenvalues for the density matrix can be computed using the relationship between it and the correlation function matrix. The correlation function matrix,

$$C_{ij} = \langle c_i^\dagger c_j \rangle, \tag{A2}$$

is determined entirely by the one particle operators. We perform a unitary rotation in the space of one particle operators,

$$S_{\alpha\beta} = \sum_{ij} \phi_\alpha^\dagger(i) c_i^\dagger \phi_\beta(j) c_j \rangle, \tag{A3}$$

where ϕ are the single particle orbitals of the free Fermi gas, plane waves. This yields the overlap matrix integrated over the spatial region for which we compute the Renyi entropies. The eigenvalues of this matrix are equivalent to those of the original C matrix. These integrals can be performed analytically for circular or strip geometries and have no dependence on spatial grid.

For this Hamiltonian we can write the density matrix as the exponential of a fictitious Hamiltonian, the entanglement Hamiltonian, with energy levels ξ_k and single particle operators a_k and $a_k^\dagger$,

$$\rho = \mathcal{K} \exp\left(-\sum_k a_k^\dagger a_k \xi_k \right). \tag{A4}$$

where $\mathcal{K}$ is a normalization constant set by $\mathrm{Tr}(\rho) = 1$. The new states, a_k are related to the eigenvectors of the correlation matrix by, $c_i = \sum_k \phi_k(i) a_k$, and the eigenvalues of the entanglement Hamiltonian are related to those of the correlation matrix, ζ_i, by,

$$\xi_i = \log\left(\frac{1-\zeta_i}{\zeta_i} \right). \tag{A5}$$

The von Neumann Entropy, S_1, is then computed as,

$$S_1 = \sum_i \ln\left(1 + \exp\left(\xi_i\right)\right) + \frac{-\xi_i}{1+\exp\left(-\xi_i\right)} \tag{A6}$$

and higher order Renyi entropies using a recursive formula,

$$\begin{aligned}
&m_0 = 0 \\
&w_0 = 1 \\
&i = 1 \\
&\text{while i} < \mathrm{N}_{tot} \\
&\quad w_i = w_{i-1}(1 + \exp\left(-\xi_i\right)) \\
&\quad m_i = m_{i-1} + \exp\left(-n\xi_i\right)(1 + m_{i-1}) \\
&\quad i = i + 1 \\
&S_n = \tfrac{1}{1-n} \log\left(\tfrac{m_{N_{tot}}+1}{(w_{N_{tot}})^n} \right)
\end{aligned} \tag{A7}$$

as shown in [36].

When computing high order Renyi entropies or the entropy of a large region, m and w can develop numerical instabilities. The normalization factor, w, and the unnormalized trace, m, contain terms that diverge as the system or Renyi entropy order, n, grows large: $w = \prod_i (1-\zeta_i)^{-1}$ and $m \sim \prod_i (1-\zeta_i)^{-n}$.

While each term diverges individually, the ratio, $r_{m,w} = \frac{m_{N_{tot}}+1}{(w_{N_{tot}})^n} \to 0$. This ratio can be written as a function of the Renyi entropies which has a known scaling form, $r_{m,w} = \exp\left((1-n)S_n\right)$. We can see that this ratio, $r_{m,w}$, scales as W^{1-n} for cylindrical geometry and $L^{(1-n)L}$ for the spherical geometry, both of which go to zero as the system size increases. This restricts the maximum size of the sub regions we can compute.